Cancer Cell
Article

Cancer Cells Display Profound Intra- and Interline Variation following Prolonged Exposure to Antimitotic Drugs

Karen E. Gascoigne[1] and Stephen S. Taylor[1,*]
[1]Faculty of Life Sciences, University of Manchester, Oxford Road, Manchester M13 9PT, UK
*Correspondence: stephen.taylor@manchester.ac.uk
DOI 10.1016/j.ccr.2008.07.002

SUMMARY

Drugs targeting the mitotic spindle are used extensively during chemotherapy, but surprisingly, little is known about how they kill tumor cells. This is largely because many of the population-based approaches are indirect and lead to vague and confusing interpretations. Here, we use a high-throughput automated time-lapse light microscopy approach to systematically analyze over 10,000 single cells from 15 cell lines in response to three different classes of antimitotic drug. We show that the variation in cell behavior is far greater than previously recognized, with cells within any given line exhibiting multiple fates. We present data supporting a model wherein cell fate is dictated by two competing networks, one involving caspase activation, the other protecting cyclin B1 from degradation.

INTRODUCTION

Microtubule toxins are used extensively during chemotherapy, demonstrating impressive efficacy in the treatment of breast and ovarian cancer (Jordan and Wilson, 2004). In addition to killing tumor cells, these cytotoxins affect normal dividing cells, causing myelosuppression (McGuire et al., 1989). While this side effect is clinically manageable, more problematic are the peripheral neuropathies caused by inhibiting microtubule dynamics in nondividing cells (Rowinsky et al., 1993).

To minimize neurotoxicity, new agents are being developed that disrupt mitosis without affecting microtubules (Jackson et al., 2007). Front-runners include Eg5 kinesin inhibitors and inhibitors of mitotic kinases, such as the Auroras and Plk1 (Keen and Taylor, 2004; Bergnes et al., 2005; Strebhardt and Ullrich, 2006). Importantly, little peripheral neuropathy manifests in patients treated with Eg5 inhibitors (Tang et al., 2008; Lee et al., 2008). Whether these new agents will exert significant antitumor effects is currently under investigation.

A major unresolved issue is defining which tumors are likely to respond to these new antimitotic agents; such knowledge would allow better design of clinical trials and pave the way for patient stratification if the drugs demonstrate efficacy. Consequently, extensive effort has been directed at understanding how cultured tumor cells respond to antimitotic agents (Rieder and Maiato, 2004; Weaver and Cleveland, 2005; Jackson et al., 2007).

It is well established that antimitotic compounds activate the spindle assembly checkpoint (SAC) leading to mitotic arrest (Musacchio and Salmon, 2007). Following prolonged arrest, a number of outcomes have been described. While some cells appear to die in mitosis, others exit mitosis without dividing and return to interphase (Rieder and Maiato, 2004; Weaver and Cleveland, 2005). Once back in interphase, some lines undergo cell-cycle arrest, others die, and others rereplicate their genomes, i.e., endocycle.

Despite extensive effort, our understanding of the factors that dictate cell fate following prolonged mitotic arrest is limited. Efforts have been hampered because commonly used population-based approaches, such as flow cytometry and western blotting, generate indirect data that can be difficult to interpret (Rieder and Maiato, 2004). In addition, different studies invariably

SIGNIFICANCE

Although traditional antimitotic agents such as the taxanes show impressive clinical efficacy in the treatment of cancer, peripheral neurotoxicities caused by interfering with microtubule dynamics in nondividing cells is a limitation. A new generation of inhibitors that block mitosis without affecting microtubule dynamics are now being tested, the front-runners being inhibitors of the Eg5 kinesin. However, we still have little understanding of the mechanisms that dictate cell fate in response to either traditional antimitotic drugs or these new agents. Here, we take a systematic, single-cell-based approach to describe how different tumor cells respond to these drugs. The data set presented provides a resource and an intellectual framework for dissecting how antimitotic agents kill tumor cells.

use different combinations of cell lines, drugs, and drug concentrations, so comparing data sets is difficult. Furthermore, the terminology used is ambiguous; "slippage" and "adaptation" are widely used to describe cell fate following prolonged arrest without any clearly stated definitions.

There is evidence that cells can "slip" out of mitosis: in nontransformed retinal pigment epithelial (RPE) cells, cyclin B1 is gradually degraded during a protracted mitotic arrest, presumably reaching a threshold no longer sufficient to maintain the mitotic state, despite continued SAC signaling (Brito and Rieder, 2006). Based on this, it has been argued that vertebrate cells slip but do not "adapt." However, there are numerous reports indicating that death can occur in mitosis (Sherwood et al., 1994; Woods et al., 1995; Panvichian et al., 1998; Rieder and Maiato, 2004). Whether this also requires cyclin B1 levels to fall below a certain threshold, as opposed to requiring induction of a separate cell death pathway, is unclear.

To understand how human tumor cells respond to antimitotic agents, we have taken a systematic approach. Using automated time-lapse light microscopy, we established a single-cell-based assay and analyzed over 10,000 cells from 15 cell lines in response to different classes of antimitotic drugs. Our aim was to generate a sufficiently large data set with which to formulate hypotheses that could then be tested with more focused experiments.

RESULTS

Time-Lapse Microscopy to Determine Cell Fate

To define how cancer cells respond to antimitotic drugs, we devised a high-throughput time-lapse microscopy approach, validating it first using HeLa cells, a line commonly employed by mitosis researchers. HeLa cells were transfected with a GFP-histone H2B cDNA, and stable integrants were selected and pooled to generate a polyclonal cell line. Cells were seeded into a 96-well plate and then synchronized in early S phase using a thymidine block (Figure 1A). After 4.5 hr following release from the block, antimitotic agents were added, and fluorescence images were acquired every 5 min for 72 hr. Image sequences were then analyzed, tracking 100 individual cells to determine their behavior. In the absence of antimitotic drugs, HeLa cells underwent multiple mitoses with normal timings (see Figure S1 available online), indicating that phototoxicity is not a limitation during the time course.

Within a few hours of drug addition, virtually all of the cells entered mitosis, indicating release from the S phase block. The majority of cells then arrested for a prolonged period before undergoing one of two fates (Figure S2A). Some cells exited mitosis without any signs of division and returned to interphase, while others clearly died in mitosis (Figure 1B). Those that returned to interphase exhibited one of three fates: some died in interphase, others remained in interphase for the remainder of the experiment, and others entered a second mitosis (Figure 1B; Figure S2A). In addition to these main fates, a few other behaviors were apparent. Although rare, some cells separated their chromosomes and divided (Figure 1B); this occurred more frequently at low drug concentrations. In addition, some cells never entered mitosis, remaining in interphase for the duration of the experiment. Others died in interphase without entering mitosis (Figure S2A).

Cancer Cells Display Complex Fate Profiles

The time-lapse analysis indicated that HeLa cells do not behave in a uniform manner following prolonged mitotic arrest. Therefore, to represent the data in a manner that facilitates comparative analyses without obscuring the complexity, we plotted fate profiles for each set of 100 cells (Figure 1C). In these profiles, each horizontal line represents one cell, with the length of the line corresponding to the duration of a given behavior and the color of the line representing the behavior (see Figure S2B for more details). When treated with 30 ng/ml nocodazole, eight out of 100 HeLa cells arrested in mitosis for an average of 489 min, exited, then remained in interphase for the remainder of the experiment (subpopulation a in Figure 1C). Fifty-five cells arrested for a similar period and also exited but then endocycled, entering second and third mitoses without ever dividing (subpopulation b). Six cells arrested, exited, entered a second mitosis, exited, and then died in the subsequent interphase (subpopulation c). Thirteen cells died in interphase following exit from their first mitosis (subpopulation d). Ten cells exited and returned to interphase following the first mitosis but then died in the second mitosis (subpopulation e). Another six cells arrested for about 768 min and then died in mitosis (subpopulation f). Two cells died in interphase without entering mitosis (subpopulation g).

The fate profile in Figure 1C clearly illustrates that when treated with nocodazole, HeLa cells do not simply exhibit a singular cell fate following prolonged mitotic arrest: although about 70% of cells endocycle, other fates manifest, including death in mitosis and death in interphase. We define this phenomenon as "intraline variation." To determine whether complex fate profiles occurred with other drugs, we analyzed the effects of taxol and an Eg5 kinesin inhibitor, AZ138 (Figure S3). Whereas nocodazole prevents spindle assembly by inhibiting microtubule polymerization, taxol stabilizes microtubules and AZ138 blocks centrosome separation. Once again, the profiles were complex, with multiple fates manifesting (Figure 1C). However, in stark contrast to the nocodazole profile, HeLa cells did not endocycle with these drugs. With taxol, 73% of cells exited a prolonged mitotic arrest and then died in the following interphase. With AZ138, 83% of cells died in mitosis. Thus, although multiple fates are observed with each drug, the proportion of cells exhibiting any given fate is dramatically different. Together, these observations are striking, revealing a complex situation not previously revealed by population-based approaches.

Cancer Cells Display Profound Intraline and Interline Variation

To determine how other types of cancer cells behave when treated with antimitotic drugs, we selected a panel of seven colon cancer lines, three of which (HCT116, DLD-1, and RKO) display microsatellite instability (MIN) and four of which (HT29, SW480, SW837, and LoVo) display chromosome instability (CIN) (see Lengauer et al., 1997), plus a panel of five lung cancer lines (A549, H226, Calu6, H2030, and H1703). All were transfected with the GFP-histone H2B cDNA, and the resulting polyclonal lines were analyzed in the presence of nocodazole, taxol, and two Eg5 inhibitors, AZ138 and monastrol (Mayer et al., 1999). For the two panels of lines, we used the minimal drug concentration required to efficiently block cell division

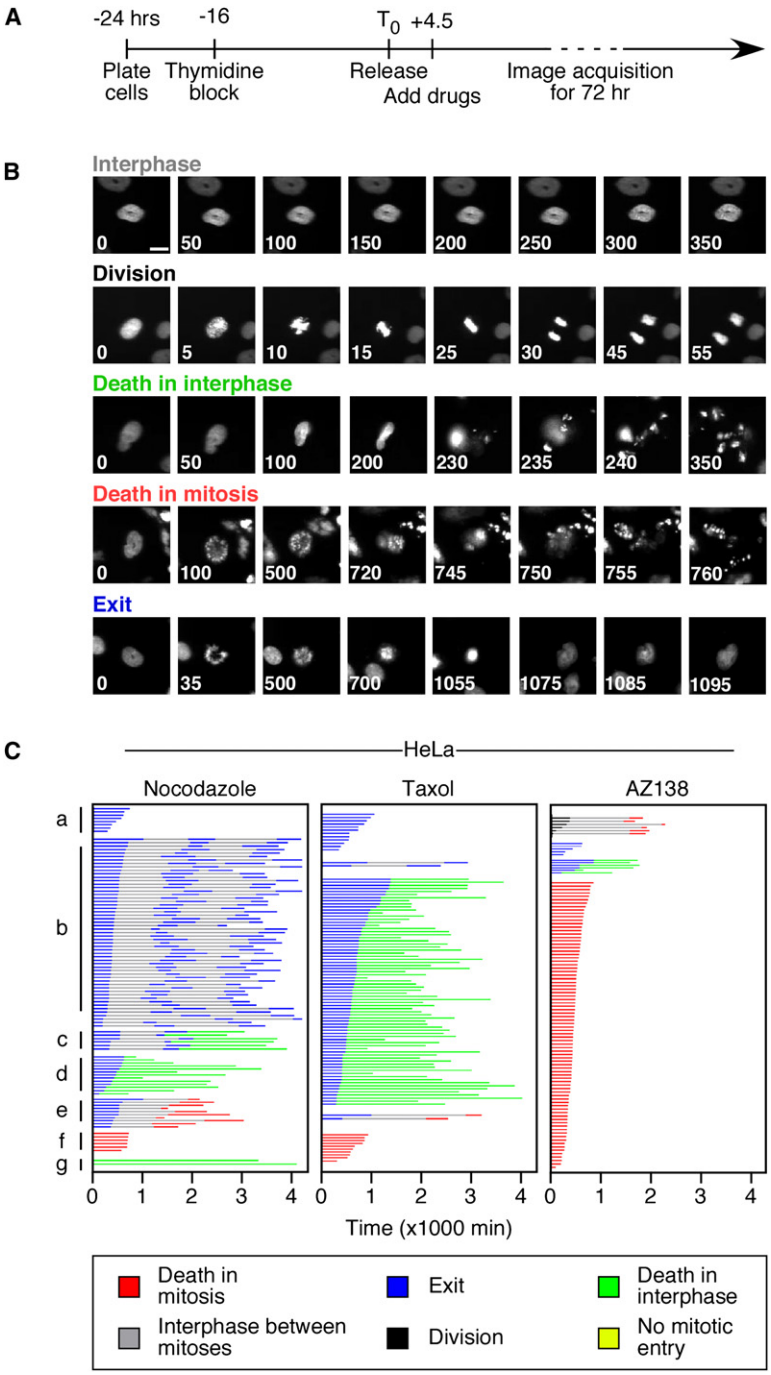

Figure 1. Time-Lapse Microscopy to Determine Cell Fate in Response to Antimitotic Agents

(A) Timeline showing experimental strategy.

(B) Examples of time-lapse sequences illustrating the fates exhibited by HeLa cells following prolonged exposure to antimitotic drugs. See text for details. Scale bar = 10 μm. Numbers indicate times in minutes.

(C) Fate profiles of HeLa cells exposed to 30 ng/ml nocodazole, 0.1 μM taxol, and 1 μM AZ138.

(Figure S4). Fate profiles were constructed for all conditions, and the full data set is presented in Figure S5. The level of complexity is profound. Cells in most lines exhibited a variety of cell fates, confirming the extensive intraline variation observed with HeLa. In addition, different cell lines exhibited dramatically different fate profiles with the same drug; we define this as "interline variation." The extent of this variation is illustrated by the MIN lines in response to 0.1 μM taxol (Figure 2A). The majority of DLD-1 cells arrested in mitosis and then returned to interphase, with 37% of these remaining in interphase and 41% entering a second mitosis. The majority of HCT116 cells also exited mitosis after prolonged arrest, but 32% then died in the subsequent interphase, a fate rarely exhibited by DLD-1. In stark contrast, virtually all of the RKO cells died in mitosis.

As outlined above, HeLa cells displayed dramatically different fate profiles with the three types of antimitotic drugs (Figure 1C). Similarly, the three MIN lines had very different fate profiles with taxol (Figure 2A). However, in contrast to HeLa, each MIN line had a more uniform response to the different drugs. For example, the majority of RKO cells died in mitosis irrespective of the drug, as did the CIN line HT29 (Figure S5). A549 provides another example of a line that shows intraline variation but less variation in response to the different drugs. With nocodazole, taxol, or AZ138, the majority of A549 cells exited mitosis without dividing, with a significant fraction then dying in interphase; very few cells endocycled or died in mitosis (Figure 2B).

In some cases, the fate profiles changed dramatically at different drug concentrations. At 200 ng/ml nocodazole, most H226 cells died in mitosis, while at 30 ng/ml, they tended to exit and return to interphase (Figure S6). H2030 cells were also sensitive to high concentrations of nocodazole, but in a different manner: at 200 ng/ml, most cells failed to enter mitosis. Paradoxically, in terms of the mitotic death phenotype, H1703 cells were more sensitive to low doses of taxol: at 0.1 μM, almost all of the cells died in mitosis, while at 10 μM, 63% returned to interphase.

Cell Fate Is Not Necessarily Genetically Predetermined

Numerous attempts have been made to identify oncogenic lesions responsible for cell fate decisions in individual lines (see Rieder and Maiato, 2004; Weaver and Cleveland, 2005). By definition, such efforts assume that different fates are genetically predetermined. However, the intraline variation revealed by our analysis argues that this is not necessarily the case. Conceivably, however, the cells within each line may not be genetically homogeneous, for example due to genetic instability and/or different integration sites of the GFP reporter. To address this, we considered A549 cells, which typically exit mitosis (only ~5% die in mitosis; Figure 2B). If these two fates were due to two genetically distinct subpopulations,

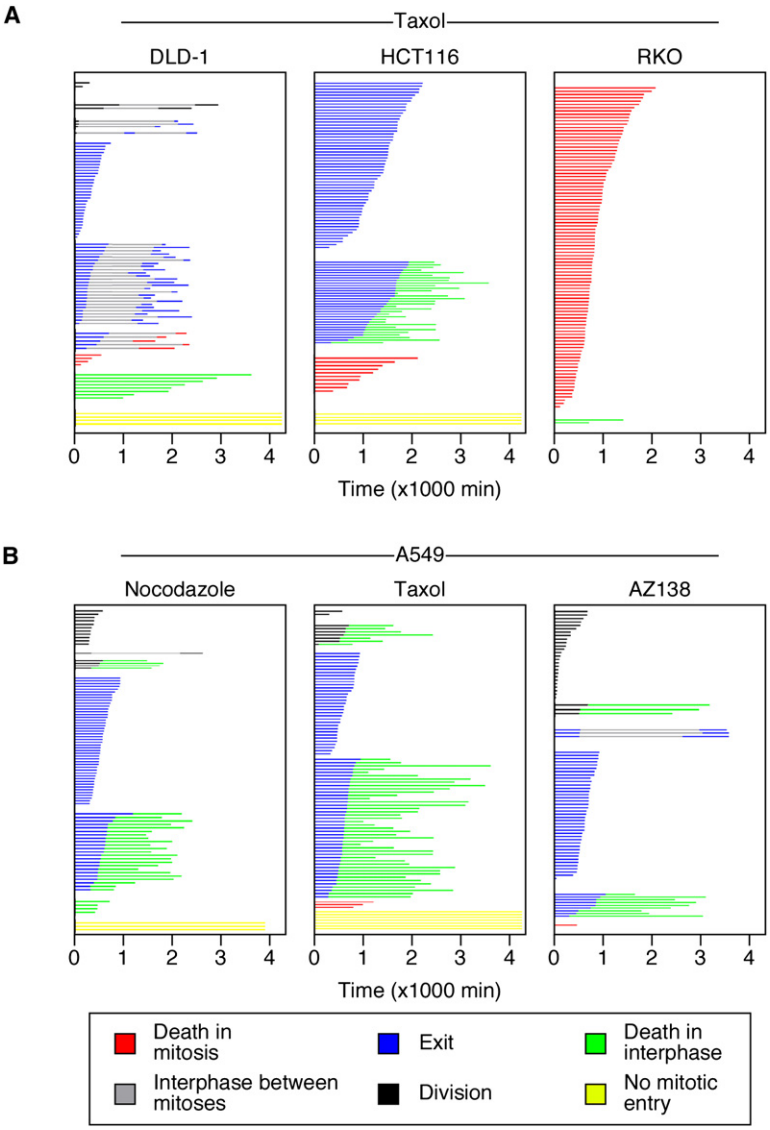

Figure 2. Inter- and Intraline Variation

(A) Fate profiles of DLD-1, HCT116, and RKO cells following exposure to 0.1 μM taxol.

(B) Fate profiles for A549 cells exposed to 30 ng/ml nocodazole, 0.3 μM taxol, and 1 μM AZ138.

then random subclones should commit to only one fate, most likely mitotic exit. However, when three subclones were exposed to nocodazole, all displayed complex fate profiles similar to the parental line (Figure S7).

To further address this, we performed a pedigree analysis. HCT116 cells were allowed to proceed through one mitosis in the absence of antimitotic drug so that we could identify daughter cells derived from the same mother. We then added AZ138 and determined the fate of 50 pairs of sisters following prolonged arrest (Figure 3). Of 12 cells that died in mitosis, only 2 sisters did so; the remaining 10 sisters exited mitosis and returned to interphase, clearly demonstrating that the fate of one sister is independent of the fate of the other.

Next, we analyzed two nontransformed cell lines that lack genomic instability and are therefore genetically more homogeneous (Kim et al., 2002). Significantly, human mammary epithelial (HME) cells also underwent multiple fates following prolonged mitotic arrest (Figure S8A). Similarly, RPE cells exhibited multiple fates, although their behavior was more homogeneous compared to the HME cells (Figure S5). Note that HME sister cells also showed different fates in the pedigree analysis (Figure S8D).

Taking together the complex fate profiles, the fact that subclones yield complex profiles typical of their parents, and the pedigree analyses, our data argue that cell fate following prolonged mitotic arrest is not determined exclusively by the genetic makeup of that cell. This clearly has significant implications for any attempts to define the genetic lesions responsible for dictating cell fate in response to antimitotic agents.

Duration of Mitotic Arrest Does Not Dictate Fate

It is widely assumed that the duration of mitotic arrest dictates subsequent cell fate (Masuda et al., 2003; Rieder and Maiato, 2004; Weaver and Cleveland, 2005; Tao et al., 2005). To test this notion, we compared the mitotic arrest period of cells that either died in mitosis or exited mitosis and returned to interphase. While the mean arrest time varied between lines and in response to different drugs, we observed no correlation between the duration of mitotic arrest and the subsequent cell fate. For example, although HCT116 cells arrested longer with taxol compared to nocodazole and AZ138, the duration of mitotic arrest was not significantly different for cells that died in mitosis versus those that exited and returned to interphase (Figure 4A). Of the HCT116 cells that exited mitosis, some remained in interphase for the remainder of the experiment, while others died. Again, there was no correlation between the time spent in mitosis and either of these postmitotic exit fates (Figure 4B). Finally, of the three lines in which cells predominantly died in mitosis, HT29 cells arrested for about 2000 min with nocodazole, taxol, and AZ138, while RKO and H1703 arrested for much shorter periods (Figure 4C). In summary, having analyzed 13 different cancer lines, we observed no obvious correlation between the duration of the mitotic arrest and the subsequent cell fate.

Chromosome Instability Is Not a Result of an Impaired Spindle Checkpoint

It is widely assumed that CIN cells have a defective or weakened SAC (Cahill et al., 1998; Masuda and Takahashi, 2002; Draviam et al., 2004; Weaver and Cleveland, 2005). Even though we previously showed that CIN cells do in fact arrest in response to spindle damage (Tighe et al., 2001), it is still believed that the SAC is somehow attenuated: although these cells arrest, they

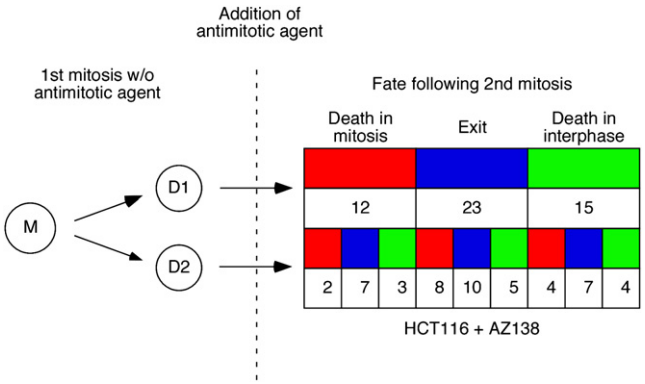

Figure 3. Cell Fate in Response to Antimitotic Drugs Is Not Genetically Predetermined

HCT116 mother cells (M) were followed through one mitosis in the absence of drug to identify pairs of daughter cells (D1 and D2). AZ138 was then added, and 50 daughter pairs were followed to determine their fate following the second mitosis, as indicated. The numbers below the colored boxes indicate the number of cells exhibiting that particular fate.

do so for a shorter time (see Weaver and Cleveland, 2005). Here, we specifically measured the time cells spent arrested in mitosis. Our data clearly show that when treated with nocodazole, taxol, or AZ138, CIN cells arrested for as long as—and even longer than, in some cases—the MIN cells (Figure 5A; Figure S9). CIN cells also arrested for longer than the nontransformed HME and RPE cells (Figure S5). The SAC is therefore clearly functional in CIN cells that experience major spindle damage. However, the SAC is capable of delaying anaphase in response to a single unaligned chromosome (Rieder et al., 1995). Therefore, we analyzed 100 cells from each of three CIN and MIN lines in the absence of drug, scoring the number of cells that entered anaphase with at least one chromosome not at the metaphase plate. In only one line—which happened to be non-CIN—did we observe a premature anaphase (Figures 5B and 5C). Note that the time-lapse assay is capable of detecting premature anaphases; when we treated DLD-1 cells with a GSK3 inhibitor to deliberately compromise the SAC (Tighe et al., 2007), we observed 12 premature events. Therefore, by the two working definitions of the SAC, namely the ability to arrest in response to spindle damage and the ability to delay anaphase in response to a single unaligned chromosome, these data clearly demonstrate that the SAC is functional in CIN cells. Thus, the notion that a weakened SAC accounts for the different fates exhibited by different cancer lines is not supported.

Chromosome Instability Is Linked to Chromosome Bridges

While a defective SAC cannot account for CIN, we were struck by two differences between the MIN and CIN lines. The first difference is that CIN cells frequently displayed chromosome bridges at anaphase (Figures 5B and 5C), confirming a recent report (Thompson and Compton, 2008). There is now compelling evidence that anaphase bridges arise because merotelic orientations (i.e., where one kinetochore is attached to both spindle poles) are not resolved prior to anaphase onset (Cimini et al., 2001). Importantly, merotelic kinetochores stably attach microtubules and therefore go undetected by the SAC. Thus, we concur that the source of CIN is not an attenuated SAC but more likely the inability to resolve merotelic orientations (Thompson and Compton, 2008). The second difference is that while both CIN and MIN cells arrest efficiently in 1 μM AZ138, only the MIN cells mounted a robust checkpoint response in 100 μM monastrol. By contrast, many of the CIN cells divided (Figure 5A). This presents a paradox: if the SAC is functional in CIN cells, why do they not arrest efficiently in monastrol?

The observation that CIN cells cannot resolve merotelics provides an explanation. Compared to AZ138, monastrol is not as potent an inhibitor of Eg5 (Figure S3); rather than a total block on centrosome separation, it therefore appears that spindles can eventually bipolarize in monastrol, allowing division (Figure 5A). Because malorientations are more likely to arise following mitotic delay (Cimini et al., 2001), merotelics are probably present despite the spindle bipolarizing. In MIN cells, we suggest that this gives rise to rounds of microtubule capture and release, thus continually generating unattached kinetochores and maintaining SAC-mediated mitotic arrest. By contrast, the inability

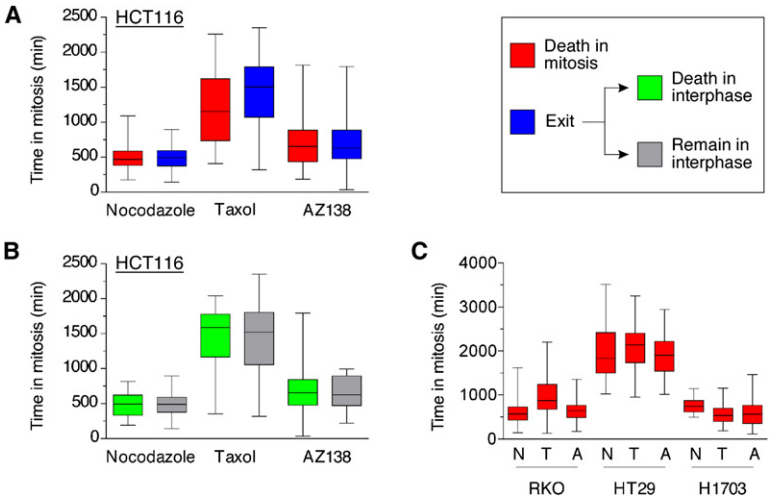

Figure 4. Duration of Mitotic Arrest Does Not Dictate Fate

Box-and-whisker plots show the time that cells spent arrested in mitosis as a function of subsequent cell fate following exposure to nocodazole (N), taxol (T), or AZ138 (A). The boxes show the mean and the interquartile ranges, while the whiskers show the full range.

(A) HCT116 cells that either died in mitosis (red) or exited mitosis and returned to interphase (blue).

(B) HCT116 cells that returned to interphase and then either died in interphase (green) or remained in interphase for the rest of the experiment (gray).

(C) RKO, HT29, and H1703 cells that died in mitosis.

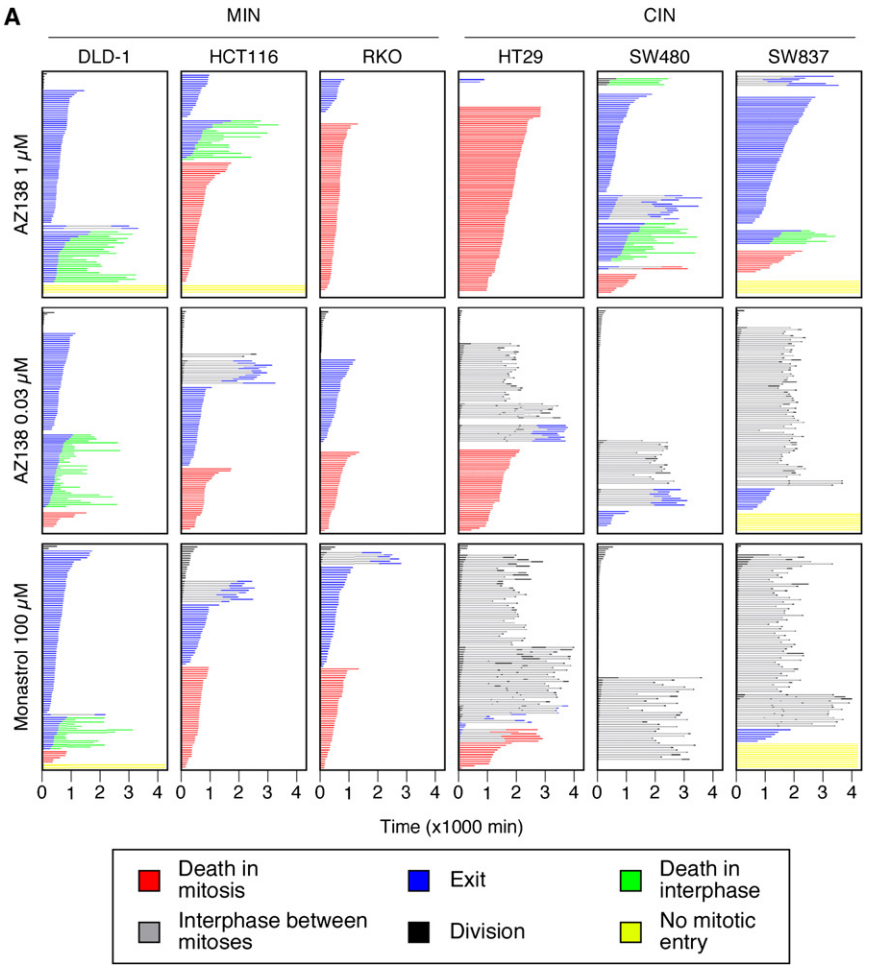

B

	Cell line	% premature anaphase	% anaphase bridges
MIN	DLD-1	0	3
	DLD-1+SB4	12	7
	HCT116	1	5
	RKO	0	0
CIN	HT29	0	24
	SW480	0	34
	SW837	0	50

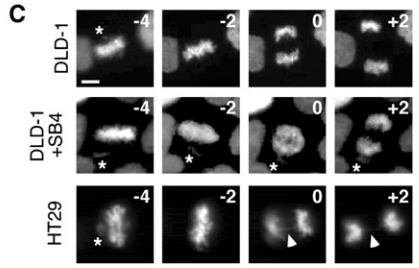

Figure 5. CIN Cells Have a Functional Spindle Checkpoint

(A) Fate profiles of three microsatellite instability (MIN) lines (DLD-1, HCT116, and RKO) and three chromosome instability (CIN) lines (HT29, SW480, and SW837) in response to 1 μM AZ138, 0.03 μM AZ138, and 100 μM monastrol.

(B) Frequency of premature anaphases and anaphase bridges in MIN and CIN cells. SB4 denotes the GSK3 inhibitor SB-415286.

(C) Time-lapse sequences showing a normal mitosis in DLD-1 cells, a premature anaphase in SB4-treated DLD-1 cells, and an anaphase bridge in HT29 cells (arrowhead). The asterisks indicate unaligned chromosomes. The numbers represent time in minutes, with t = 0 being the first frame showing signs of anaphase chromosome movement. Scale bar = 10 μm.

of CIN cells to resolve merotelics means that unattached kinetochores are not generated. The SAC therefore becomes satisfied, permitting cell-cycle progression. Consistent with this hypothesis, colon cancer cells can form bipolar spindles in the presence of monastrol (Figure S10B). Furthermore, kinetochores on bipolar spindles in monastrol-treated DLD-1 cells (MIN) stained strongly for Bub1, consistent with malorientations and checkpoint activation (Figure S10C). By contrast, kinetochores in HT29 and SW480 cells (both CIN) stained weakly for Bub1. This hypothesis predicts that at a low concentration of AZ138, yielding a level of Eg5 inhibition equivalent to that achieved with 100 μM monastrol, the MIN-CIN differential should also manifest. Indeed, at 0.03 μM AZ138, the MIN cells arrested while the CIN cells frequently divided (Figure 5A; see also Figure S10).

Although many CIN cells divide following low-penetrance Eg5 inhibition, they probably do so aberrantly: while 64% of untreated HT29 cells completed three divisions within 72 hr (data not shown), only 8% did so in 0.03 μM AZ138 (Figure 5A). In addition, the majority of SW480 cells arrested after their first division in the presence of AZ138. While this raises the possibility that CIN cells may be more sensitive to transient Eg5 inhibition, it is not because they have an attenuated SAC but because they cannot resolve malorientations.

Cell Fate and the Spindle Checkpoint

Several reports argue that the different fates of CIN cells following prolonged mitotic arrest arise due to differences in SAC status (Kasai et al., 2002; Wang et al., 2003; Vogel et al., 2004; Lee et al., 2004; Sudo et al., 2004; Tao et al., 2007). However, as we show, the SAC is not defective in CIN cells. This is not to say that the SAC is not required for the long-term response to antimitotic drugs; artificially attenuating the SAC in HeLa cells does alter the postmitotic response (e.g., Taylor and McKeon, 1997). Indeed, whether a cell dies in mitosis or dies in the subsequent interphase, the SAC is required (Figure S11). When treated with taxol, DLD-1 cells typically exit mitosis and arrest in interphase while HT29 cells die in mitosis. However, when we attenuated the SAC using the Aurora B inhibitor ZM447439 (Ditchfield et al., 2003), virtually all of the cells in both lines endocycled (Figure S11). Thus, both death in mitosis and the postmitotic response require SAC function. This does not, however, imply that the SAC "talks" directly to the signaling pathways that cause mitotic death or control postmitotic cell fate, as is often suggested (e.g., Shin et al., 2003; Niikura et al., 2007). The simplest explanation is that prolonged mitotic

arrest—which is dependent on the SAC—activates cell death pathways. A key question, therefore, is how prolonged mitotic arrest activates the cell death machinery.

Death in Mitosis Is Caspase Dependent

It was recently reported that mitotic death of HeLa cells exposed to antimitotic drugs is caspase independent (Niikura et al., 2007). To determine whether this is true for other cancer cells, we determined the fate profiles for HCT116, RKO, HT29, and Calu6 cells in the presence of antimitotic drugs plus a pan-caspase inhibitor. In all cases, the caspase inhibitor shifted the fate profile, reducing the number of cells that died in mitosis in favor of cells that exited and returned to interphase (Figure S5). For example, in the presence of AZ138, 57 HCT116 cells died in mitosis; upon caspase inhibition, this was reduced to 12 (Figure 6A). HT29 cells typically die in mitosis with all antimitotic drugs. Upon caspase inhibition, the majority of HT29 cells exited mitosis and returned to interphase (Figure S5). Thus, caspase-independent mitotic cell death does not appear to be a universal feature of cancer cells. Strikingly, caspase inhibition often prolonged the duration of the mitotic arrest. Mitotic cell death in HCT116 cells exposed to AZ138 occurred, on average, after 761 ± 62 min (Figure 6B). This was extended to 1627 ± 57 min in the presence of the caspase inhibitor. Likewise, cells that returned to interphase also spent longer in mitosis when treated with the caspase inhibitor (Figure 6B). However, for those cells that exited mitosis and then died in interphase, the caspase inhibitor did not prolong the time between mitotic exit and cell death (Figure 6B). HME cells behaved similarly when treated with the caspase inhibitor (Figures S8B and S8C).

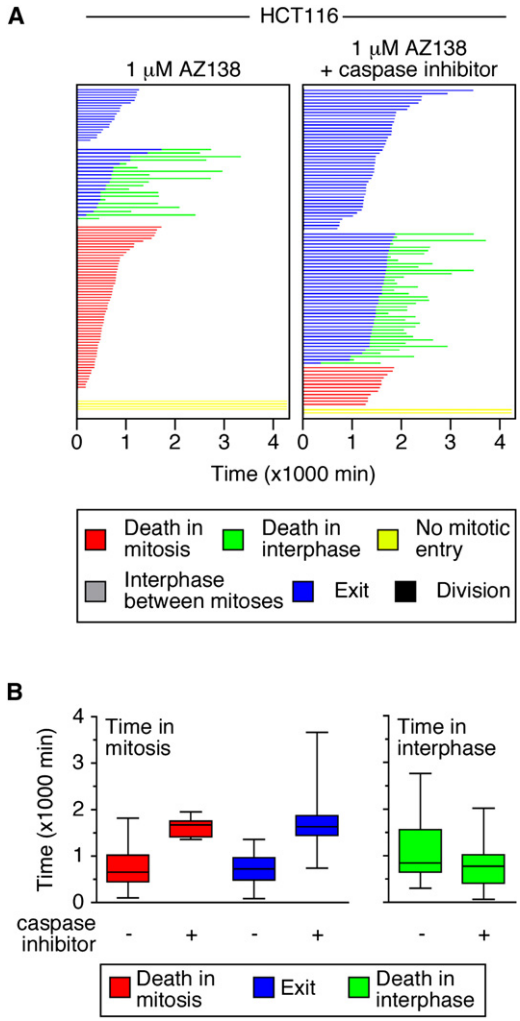

Figure 6. Death in Mitosis Is Caspase Dependent

(A) Fate profiles of HCT116 cells treated with 1 μM AZ138 without or with the pan-caspase inhibitor Boc-D-FMK.

(B) Box-and-whisker plots showing the time in mitosis (left panel) and time in interphase (right panel) as a function of subsequent cell fate. The left panel shows HCT116 cells that either died in mitosis (red) or exited mitosis and returned to interphase (blue). The right panel shows the duration of interphase after mitotic exit and before subsequent cell death (green). The boxes show the mean and the interquartile ranges, while the whiskers show the full range.

Delaying Slippage Shifts the Fate Profile to Death in Mitosis

The observation that cyclin B1 is slowly degraded in RPE cells during a prolonged mitosis has led to the suggestion that vertebrate cells "slip" but do not "adapt" (Brito and Rieder, 2006). However, because caspase inhibition extends the arrest time and shifts the fate profile (Figure 6), cyclin B1 degradation cannot be the only mechanism at play here. Rather, we speculated that cell fate is dictated by two competing but independent mechanisms, one involving caspase activation, the other protecting cyclin B1 from degradation. Thus, by slowing down caspase activation, mitotic cell death in HCT116 cells is delayed, and thus the cells stay in mitosis for longer. During this time, cyclin B1 continues to be slowly degraded, eventually allowing slippage. In other words, delaying apoptosis allows more time for slippage. If this is the case, the converse should also be true: delaying slippage should allow more time for death signals to accumulate.

To test this, we generated a DLD-1 cell line expressing either GFP or GFP-tagged cyclin B1 (Figure S12A). Whereas GFP was relatively stable during an unperturbed mitosis, GFP-cyclin B1 was degraded prior to anaphase, validating it as a slippage marker (Figure 7B). Consistent with delaying slippage, overexpression of GFP-cyclin B1 extended the duration that cells arrested in mitosis when challenged with AZ138 (Figure 7A). Strikingly, the fate profile also shifted markedly: whereas only 6 cells expressing GFP died in mitosis, 54 cells expressing GFP-cyclin B1 did so (Figure 7A). Thus, delaying slippage does indeed provide more time to accumulate death signals.

Cells that Die in Mitosis Do Not Breach the Exit Threshold

Our observations are consistent with the notion that delaying caspase activation allows more time for slippage (Figure 6) and that, conversely, delaying cyclin B1 degradation allows more time for death signals to accumulate (Figure 7A). This provides a possible explanation for intraline variation. Perhaps cells that exit do so because cyclin B1 falls below the threshold required to maintain mitosis before sufficient death signals accumulate. Conversely, cells that die in mitosis accumulate

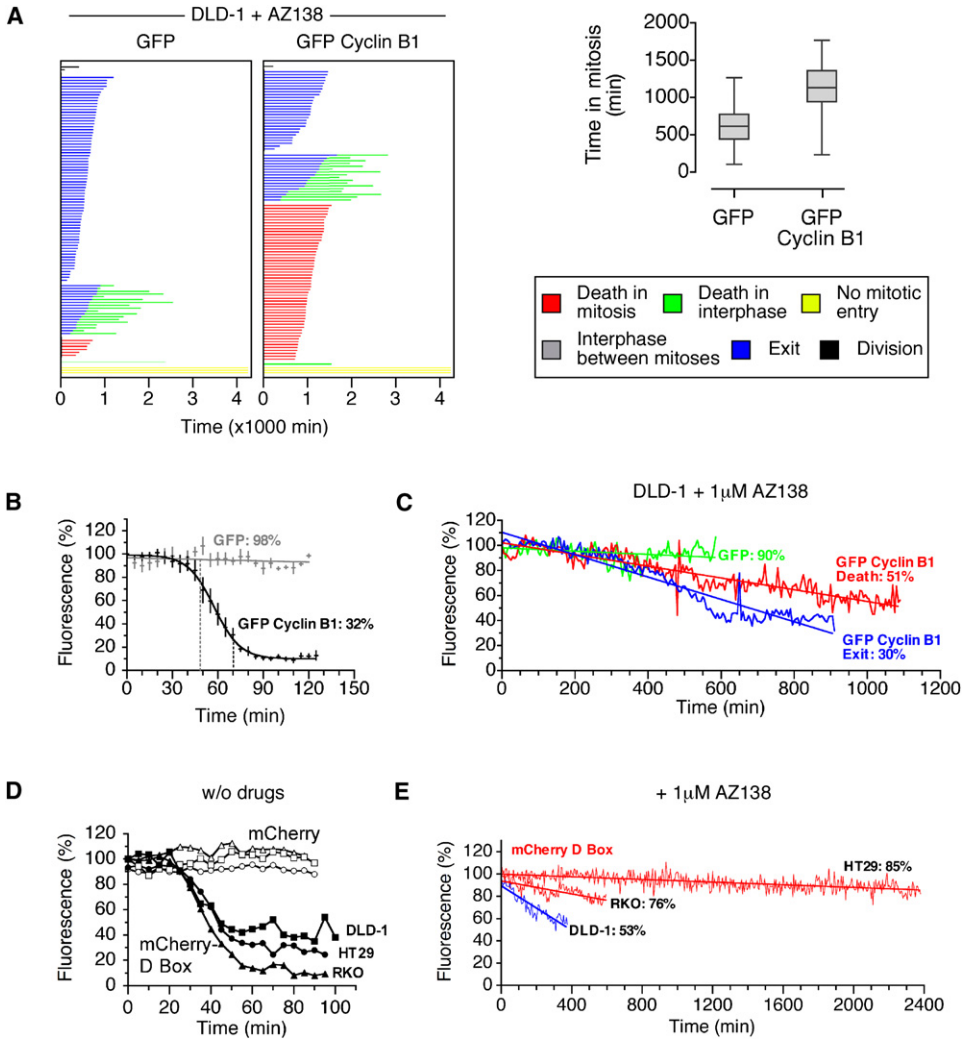

Figure 7. Delaying Slippage Promotes Death in Mitosis

(A) Left panel: fate profiles of DLD-1 cells expressing either GFP or GFP-tagged cyclin B1. Right panel: box-and-whisker plots showing that expression of GFP-cyclin B1 extends the duration of mitotic arrest in response to AZ138. The boxes show the mean and the interquartile ranges, while the whiskers show the full range.

(B) Degradation kinetics of GFP-cyclin B1 during an unperturbed mitosis. t = 0 marks nuclear envelope breakdown, and dashed vertical lines indicate anaphase onset. The graph shows the mean fluorescence from six cells ± SEM.

(C) Fluorescence intensities of DLD-1 cells expressing GFP-cyclin B1 that either died in mitosis (red) or exited (blue) in the presence of 1 μM AZ138. Values represent the mean of six cells.

(D) Degradation kinetics of mCherry (white symbols) or mCherry D box (black symbols) during unperturbed mitoses in DLD-1 (squares), HT29 (circles), and RKO (triangles). t = 0 marks nuclear envelope breakdown. The graph shows the mean fluorescence from five cells.

(E) Fluorescence intensities of DLD-1, HT29, and RKO cells expressing an mCherry D box fusion. Values represent the mean of six cells.

sufficient death signals before cyclin B1 levels reach the threshold. To test this, we quantitated GFP-cyclin B1 signal intensity in six DLD-1 cells that exited in the presence of AZ138 and six that died in mitosis. Note that in the absence of drug, anaphase occurred when GFP-cyclin B1 levels fell to ~32% (Figure 7B), defining the threshold. In cells that died in mitosis, GFP-cyclin B1 levels fell to ~51%, while in those that exited, it fell to ~30%. (Figure 7C). Thus, cells that exit mitosis do so because cyclin B1 levels breach the mitotic exit threshold. By contrast, in cells that die in mitosis, cyclin B1 levels do not fall below the mitotic exit threshold.

In turn, these observations may help explain interline variation. Perhaps in lines that predominantly die in mitosis, such as RKO and HT29, the level of cyclin B1 never approaches the mitotic exit threshold. To test this, we generated RKO, HT29, and DLD-1 lines expressing cyclin B1's D box fused to mCherry (Figure S12B). This allowed us to monitor cyclin degradation without elevating Cdk1 activity. In the absence of drug, mCherry D box levels in RKO and HT29 cells fell to ~45% by anaphase onset (Figure 7D), thus defining the threshold required for mitotic exit. In DLD-1 cells, the threshold was slightly higher at ~60%. Significantly, when treated with

AZ138, mCherry D box levels only fell to 85% in HT29 and 76% in RKO cells before these cells died (Figure 7E). Thus, in these two lines, cyclin B1 degradation is slow and does not approach the threshold required for mitotic exit. By contrast, DLD-1 cells degraded the mCherry D box much faster, its level falling to 53% in under 400 min (Figure 7E), explaining their tendency to exit mitosis.

DISCUSSION

Our analysis reveals a level of complexity that is at first overwhelming. While some degree of interline variation was anticipated, it is striking that cells within a line can exhibit multiple fates. This intraline variation does not appear to be genetically predetermined, because sisters can undergo different fates. Despite the complexity, we can rule out two preexisting hypotheses. First, cell fate does not correlate with the duration of mitotic arrest. Second, cell fate is not determined by differences in the status of the spindle checkpoint. More importantly, delaying caspase activation or delaying cyclin B1 degradation dramatically alters the fate profiles, allowing us to formulate a model explaining both intra- and interline variation.

The Perils of Population Analyses

The intraline variation exposed here provides an explanation as to why population-based studies lead to vague and confusing interpretations (Rieder and Maiato, 2004). Sensitive immunoblotting techniques can easily detect activation of a particular signaling pathway, even if only a small fraction of cells within the population have triggered that pathway. This subpopulation may be obscured in a complex flow cytometry profile, resulting in erroneous correlations between DNA content histograms and molecular events measured on blots. By contrast, time-lapse tracking of individual living cells has allowed us to directly correlate mitotic arrest times and cell fate. Clearly, our approach is not entirely noninvasive, and it is conceivable that the GFP imaging procedure affects cellular behavior. However, phototoxicity does not appear to be limiting (Figure S1). Furthermore, bright-field imaging and flow cytometry-based experiments (data not shown) support the data described here. In addition, a comprehensive single-cell immunofluorescence-based study reveals a level of complexity consistent with that described here (Shi et al., 2008).

Cell Fate Is Dictated by Competing Networks

Having exposed the true extent of the variation exhibited by cells in response to antimitotic agents, only now can we start to devise meaningful hypotheses. First, however, we need to define several terms. We will use "slippage" to describe the process by which a cell exits a prolonged mitotic arrest when cyclin B1 levels fall below the threshold required to maintain the mitotic state (Brito and Rieder, 2006). To describe the process by which a cell activates a death pathway while still in mitosis, we will use the phrase "death in mitosis." To describe cell-cycle arrest and/or apoptosis of interphase cells following slippage, we will use the term "postmitotic response." Accordingly, efficient entry into a new cell cycle following slippage indicates the lack of a robust postmitotic response.

We propose that cell fate is dictated by two competing but independent networks, one involving activation of cell death pathways, the other protecting cyclin B1 from degradation (Figure 8). During prolonged mitotic arrest, these two networks work in opposite directions: while cell death signals become stronger, cyclin B1 levels fall. We suggest that both networks have thresholds and that the fate of the cell is dictated by which threshold is breached first. Thus, if cyclin B1 levels fall below the mitotic exit threshold first, slippage occurs (Figure 8A). If the death threshold is breached first, the cell dies in mitosis.

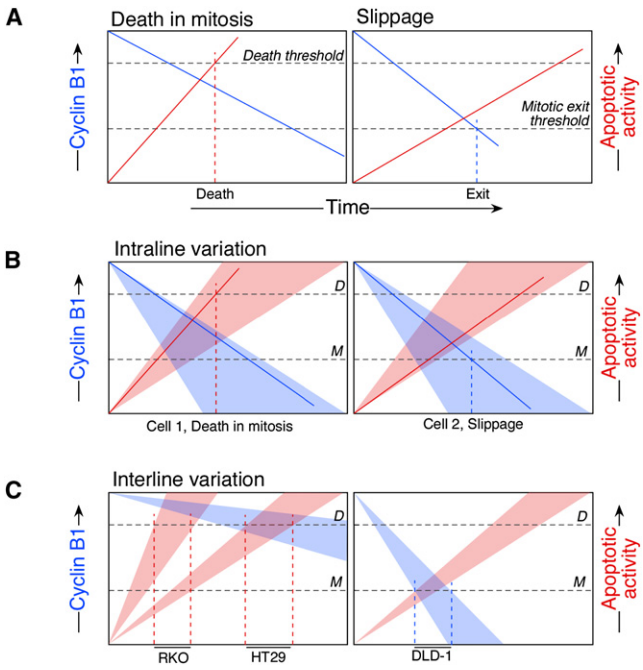

Figure 8. Model Explaining Intra- and Interline Variation
(A) Death in mitosis versus slippage.
(B) Intraline variation.
(C) Interline variation.

This model helps explain both intra- and interline variation. Although the genetic background of a particular cell line places limits on rates and thresholds, for cells within any given line, network stability will vary from cell to cell. Consequently, rates of cyclin B1 degradation and caspase activation probably occupy broad ranges (Figure 8B). Because the two competing networks are independent, the first threshold breached may therefore vary from cell to cell, thus explaining intraline variation. With respect to interline variation, for lines whose cells predominantly die in mitosis, e.g., HT29 and RKO, differences in genetic background result in relatively slow rates of cyclin B1 degradation, and thus the cell death threshold is invariably breached first (Figure 8C). However, cell death signals may accumulate faster in RKO compared to HT29, accounting for different durations of mitotic arrest before death. By contrast, in a line where cells rarely die in mitosis, e.g., DLD-1, the mitotic exit threshold is invariable breached first (Figure 8C).

A key issue now is to determine the molecular parameters governing network output, namely the rates and thresholds. Although silencing of the SAC triggers cyclin B1 degradation during a normal mitosis, the SAC is only part of the network controlling cyclin B1 degradation during a protracted mitosis;

other variables will be defined by processes downstream of the SAC such as the balance of ubiquitination and deubiquitination of cyclin B1. Factors influencing caspase activation during mitosis are less well understood, but a key player could be caspase-9, which was recently shown to be phosphorylated by Cdk1 in order to restrain apoptosis during mitosis (Allan and Clarke, 2007). Our model is consistent with Allan and Clarke's notion that death in mitosis may be induced by the slow net dephosphorylation of caspase-9. The nature of the damage signal is still elusive. One possibility is that DNA damage slowly accumulates during a protracted mitosis that, in the absence of efficient repair, eventually activates intrinsic apoptotic pathways.

Drug-Dependent and Concentration-Dependent Variation

Our model accounts for variation with respect to whether a cell dies in mitosis or exits and returns to interphase. It does not, however, explain why HeLa cells for example display different fate profiles with different drugs. Recently, the phosphorylation status of the anaphase-promoting complex/cyclosome (APC/C), purified from HeLa cells, has been determined by quantitative mass spectroscopy (Steen et al., 2008). The APC/C, an E3 ubiquitin ligase responsible for targeting cyclin B1 for degradation and thus triggering mitotic exit, is the downstream target of the SAC (Musacchio and Salmon, 2007). Interestingly, the phosphorylation profiles vary depending on the antimitotic drug used to arrest the cells in mitosis (Steen et al., 2008). The reason for this is unclear but could involve differential effects on microtubule dynamics and/or polymer levels. The different fate profiles exhibited by HeLa cells may therefore be due to differential APC/C phosphorylation. In addition, the spectrum of APC/C phosphorylation may depend on drug concentration, explaining why the fate of some lines varies at different drug concentrations (Figure S5). If differential APC/C phosphorylation does indeed dictate fate, then lines that behave similarly with different drugs and/or at different concentrations should have more uniform APC/C phosphorylation profiles. While experiments testing these predictions will not be straightforward, they may provide critical insight into the mechanisms dictating the rate of cyclin B1 degradation during a protracted mitosis.

The Postmitotic Response

Another aspect of variation not immediately covered by our model is cell fate following slippage, i.e., the postmitotic response. The factors at play here remain obscure, and it is not even clear whether the postmitotic response is a delayed reaction to damage incurred during mitosis or whether returning to interphase without successfully dividing creates a de novo damage signal. The concept of a "tetraploidy checkpoint" assumes that an aberrant division creates a de novo damage signal, namely tetraploidy (Andreassen et al., 2001). However, it is important to note that cell division failure is not sufficient to provoke a postmitotic response: artificially abrogating the SAC in the presence of antimitotic drugs causes cell division to fail, yet the cell cycle continues (Taylor and McKeon, 1997). Indeed, the "tetraploidy checkpoint" concept is no longer favored, as the cell-cycle arrest observed can be accounted for by drug-induced DNA damage (Uetake and Sluder, 2004). Thus, the postmitotic response may simply be a delayed reaction to damage incurred during mitosis. If this is the case, then two additional observations allow our model to be extended to account for the postmitotic variation. First, the time between mitotic exit and death in interphase was variable and did not correlate with time spent in mitosis (Figure 4B). Second, the caspase inhibitor did not extend the gap between mitotic exit and subsequent apoptosis (Figure 6B). It is therefore possible that in some cells, sufficient damage accumulates during mitosis to initiate apoptosis but execution is delayed. Because the networks governing slippage and death in mitosis are not linked, cyclin B1 degradation continues regardless, allowing some cells to slip out of mitosis prior to executing the apoptotic program. Apoptosis would manifest in the subsequent interphase at a time linked to initiation but not to mitotic exit.

Note that we do not exclude the possibility that there is a separate postmitotic response. We previously showed that p53 is required to restrain endocycling when cells exit mitosis in the presence of an Aurora B inhibitor (Ditchfield et al., 2003). In this case, although cell division fails, mitotic exit is delayed only briefly; there is no protracted mitotic arrest. It seems unlikely that this brief delay is sufficient for damage signals to accumulate to a level high enough to trigger a response, strongly suggesting that there is indeed a separate, p53-dependent postmitotic response. While the nature of the damage signal is elusive, it is not clear to us that there is any evidence for a de novo trigger. It has been suggested that p53 is activated during a prolonged mitotic arrest (Vogel et al., 2004), but there is no direct evidence for this. In our experiments, while inhibiting p53 allowed more endocycling, it did not protect against mitotic death (Figure S13). One possibility is that even minor perturbations during mitosis induce DNA damage or other forms of cellular stress that, while insufficient to trigger death in mitosis, may be sufficient to activate p53 and/or other responses in the subsequent interphase. The caspase-9 data provide insight here (Allan and Clarke, 2007): perhaps mitosis-specific events, such as caspase-9 phosphorylation, raise a threshold that allows minor insults to be ignored. Upon return to interphase, the threshold is lowered, e.g., by caspase-9 dephosphorylation, allowing the damage to be sensed. If this is the case, the postmitotic response need not be any different from the normal interphase mechanisms that respond to cell stresses.

Future Directions

The analysis described here illustrates that high-throughput time-lapse approaches offer advantages over less direct approaches. However, this type of analysis is currently limited because there are few bioprobes capable of monitoring molecular events in living cells. Developing such tools will be essential in order to decode the mechanisms that dictate cell fate in response to antimitotic agents.

EXPERIMENTAL PROCEDURES

Cell Lines and Drugs

Lung carcinoma lines (A549, H226, Calu6, H2030, and H1703) and colon carcinoma lines (DLD-1, HCT116, RKO, HT29, SW480, SW837, and LoVo) were obtained from the American Type Culture Collection. hTERT-HME and hTERT-RPE were from Clontech, and TA-HeLa cells were as described previously (Taylor and McKeon, 1997). All cancer lines and hTERT-RPE were cultured in DMEM plus 10% fetal calf serum (GIBCO), 2 mM glutamine, 100 U/ml

penicillin, and 100 U/ml streptomycin (Lonza), while hTERT-HME cells were cultured in mammary epithelial growth medium (Lonza). All lines were grown at 37°C in a humidified 5% CO_2 incubator. Small molecules dissolved in DMSO were used at the following concentrations unless stated otherwise: nocodazole (Sigma) 30 ng/ml, taxol (Sigma) 0.1 μM, AZ138 (AstraZeneca) 1 μM, monastrol (Sigma) 100 μM, SB-415286 (Calbiochem) 30 μM, ZM447439 (Tocris) 2 μM, Boc-D-FMK (Calbiochem) 100 μM. Thymidine dissolved in water was used at 2 mM.

Retroviral Infections and Transfections

A GFP-tagged histone H2B cDNA (Morrow et al., 2005) cloned into a pLPCX-based vector (Clontech) was introduced into all of the cell lines using retrovirus-mediated transduction as described previously (Hussein and Taylor, 2002). Stably transduced cells were selected in puromycin, and colonies were pooled and expanded to create polyclonal cell lines. cDNAs encoding the N-terminal 90 amino acids of cyclin B1 fused to mCherry and p53 (wild-type and V143A) were cloned into a pLNCX2-based vector (Clontech) modified to contain an N-terminal Myc tag, then similarly transduced into cells followed by selection in G418. Isogenic DLD-1 cells expressing GFP-tagged cyclin B1 under tetracycline control were generated using FRT-Flp-based recombination as described previously (Tighe et al., 2004).

Time-Lapse Imaging

Cells were seeded in 96-well μClear plates (Greiner) at 1.3×10^4 cells per well in a volume of 200 μl. Eight hours later, thymidine was added for 16 hr. Cells were then washed three times in PBS and released in 100 μl of fresh medium for 4.5 hr before addition of drugs in another 100 μl of medium. Imaging was performed using a Pathway Bioimager 855 (BD biosciences) with a 20×/0.30 UPlan FLN objective, with images collected every 5 min using a 0.1 s exposure. Image sequences were viewed using NIH ImageJ software (http://rsbweb.nih.gov/ij/), and cell behavior was analyzed manually. For pedigree analysis, cells were imaged in drug-free medium for 16 hr; drug-containing medium was then added, and image acquisition was continued for a further 72 hr. To monitor chromosome segregation in the absence of drug and to quantitate degradation of fluorescently tagged fusions, cells were seeded in 24-well plates (Corning) at 3×10^4 cells per well and then synchronized with thymidine as above. After drug addition, image acquisition was performed using a Zeiss Axiovert 200-based system as described previously (Morrow et al., 2005). Images were collected every 5 min using a 32× Apoplan objective. Image sequences were viewed and integrated pixel intensity measurements were performed using ImageJ.

SUPPLEMENTAL DATA

The Supplemental Data include thirteen figures and can be found with this article online at http://www.cancercell.org/cgi/content/full/14/2/111/DC1/.

ACKNOWLEDGMENTS

We thank Dennis Huszar (AstraZeneca) for AZ138 and comments on the manuscript; Jonathon Pines (University of Cambridge) and David Lane (University of Dundee) for cyclin B1 and p53 cDNAs, respectively; Stephen Doxsey (University of Massachusetts) for RPE cells; Peter March for help with microscopy; and Claudia Wellbrock plus members of the Taylor laboratory for comments on the manuscript. The Pathway Bioimager 855 microscope was purchased with funds from the University of Manchester Strategic Fund. K.E.G. is funded by a studentship from the BBSRC, and S.S.T. is a Cancer Research UK Senior Fellow. This work was funded in part by AstraZeneca.

Received: May 15, 2008
Revised: June 27, 2008
Accepted: July 7, 2008
Published online: July 24, 2008

REFERENCES

Allan, L.A., and Clarke, P.R. (2007). Phosphorylation of caspase-9 by CDK1/cyclin B1 protects mitotic cells against apoptosis. Mol. Cell *26*, 301–310.

Andreassen, P.R., Lohez, O.D., Lacroix, F.B., and Margolis, R.L. (2001). Tetraploid state induces p53-dependent arrest of nontransformed mammalian cells in G1. Mol. Biol. Cell *12*, 1315–1328.

Bergnes, G., Brejc, K., and Belmont, L. (2005). Mitotic kinesins: prospects for antimitotic drug discovery. Curr. Top. Med. Chem. *5*, 127–145.

Brito, D.A., and Rieder, C.L. (2006). Mitotic checkpoint slippage in humans occurs via cyclin B destruction in the presence of an active checkpoint. Curr. Biol. *16*, 1194–1200.

Cahill, D.P., Lengauer, C., Yu, J., Riggins, G.J., Willson, J.K., Markowitz, S.D., Kinzler, K.W., and Vogelstein, B. (1998). Mutations of mitotic checkpoint genes in human cancers. Nature *392*, 300–303.

Cimini, D., Howell, B., Maddox, P., Khodjakov, A., Degrassi, F., and Salmon, E.D. (2001). Merotelic kinetochore orientation is a major mechanism of aneuploidy in mitotic mammalian tissue cells. J. Cell Biol. *153*, 517–527.

Ditchfield, C., Johnson, V.L., Tighe, A., Ellston, R., Haworth, C., Johnson, T., Mortlock, A., Keen, N., and Taylor, S.S. (2003). Aurora B couples chromosome alignment with anaphase by targeting BubR1, Mad2, and Cenp-E to kinetochores. J. Cell Biol. *161*, 267–280.

Draviam, V.M., Xie, S., and Sorger, P.K. (2004). Chromosome segregation and genomic stability. Curr. Opin. Genet. Dev. *14*, 120–125.

Hussein, D., and Taylor, S.S. (2002). Farnesylation of Cenp-F is required for G2/M progression and degradation after mitosis. J. Cell Sci. *115*, 3403–3414.

Jackson, J.R., Patrick, D.R., Dar, M.M., and Huang, P.S. (2007). Targeted anti-mitotic therapies: can we improve on tubulin agents? Nat. Rev. Cancer *7*, 107–117.

Jordan, M.A., and Wilson, L. (2004). Microtubules as a target for anticancer drugs. Nat. Rev. Cancer *4*, 253–265.

Kasai, T., Iwanaga, Y., Iha, H., and Jeang, K.T. (2002). Prevalent loss of mitotic spindle checkpoint in adult T-cell leukemia confers resistance to microtubule inhibitors. J. Biol. Chem. *277*, 5187–5193.

Keen, N., and Taylor, S. (2004). Aurora-kinase inhibitors as anticancer agents. Nat. Rev. Cancer *4*, 927–936.

Kim, H., Farris, J., Christman, S.A., Kong, B.W., Foster, L.K., O'Grady, S.M., and Foster, D.N. (2002). Events in the immortalizing process of primary human mammary epithelial cells by the catalytic subunit of human telomerase. Biochem. J. *365*, 765–772.

Lee, C.W., Belanger, K., Rao, S.C., Petrella, T.M., Tozer, R.G., Wood, L., Savage, K.J., Eisenhauer, E.A., Synold, T.W., Wainman, N., and Seymour, L. (2008). A phase II study of ispinesib (SB-715992) in patients with metastatic or recurrent malignant melanoma: a National Cancer Institute of Canada Clinical Trials Group trial. Invest. New Drugs *26*, 249–255.

Lee, E.A., Keutmann, M.K., Dowling, M.L., Harris, E., Chan, G., and Kao, G.D. (2004). Inactivation of the mitotic checkpoint as a determinant of the efficacy of microtubule-targeted drugs in killing human cancer cells. Mol. Cancer Ther. *3*, 661–669.

Lengauer, C., Kinzler, K.W., and Vogelstein, B. (1997). Genetic instability in colorectal cancers. Nature *386*, 623–627.

Masuda, A., and Takahashi, T. (2002). Chromosome instability in human lung cancers: possible underlying mechanisms and potential consequences in the pathogenesis. Oncogene *21*, 6884–6897.

Masuda, A., Maeno, K., Nakagawa, T., Saito, H., and Takahashi, T. (2003). Association between mitotic spindle checkpoint impairment and susceptibility to the induction of apoptosis by anti-microtubule agents in human lung cancers. Am. J. Pathol. *163*, 1109–1116.

Mayer, T.U., Kapoor, T.M., Haggarty, S.J., King, R.W., Schreiber, S.L., and Mitchison, T.J. (1999). Small molecule inhibitor of mitotic spindle bipolarity identified in a phenotype-based screen. Science *286*, 971–974.

McGuire, W.P., Rowinsky, E.K., Rosenshein, N.B., Grumbine, F.C., Ettinger, D.S., Armstrong, D.K., and Donehower, R.C. (1989). Taxol: a unique antineoplastic agent with significant activity in advanced ovarian epithelial neoplasms. Ann. Intern. Med. *111*, 273–279.

Morrow, C.J., Tighe, A., Johnson, V.L., Scott, M.I., Ditchfield, C., and Taylor, S.S. (2005). Bub1 and aurora B cooperate to maintain BubR1-mediated inhibition of APC/CCdc20. J. Cell Sci. *118*, 3639–3652.

Musacchio, A., and Salmon, E.D. (2007). The spindle-assembly checkpoint in space and time. Nat. Rev. Mol. Cell Biol. *8*, 379–393.

Niikura, Y., Dixit, A., Scott, R., Perkins, G., and Kitagawa, K. (2007). BUB1 mediation of caspase-independent mitotic death determines cell fate. J. Cell Biol. *178*, 283–296.

Panvichian, R., Orth, K., Day, M.L., Day, K.C., Pilat, M.J., and Pienta, K.J. (1998). Paclitaxel-associated multimininucleation is permitted by the inhibition of caspase activation: a potential early step in drug resistance. Cancer Res. *58*, 4667–4672.

Rieder, C.L., and Maiato, H. (2004). Stuck in division or passing through: what happens when cells cannot satisfy the spindle assembly checkpoint. Dev. Cell *7*, 637–651.

Rieder, C.L., Cole, R.W., Khodjakov, A., and Sluder, G. (1995). The checkpoint delaying anaphase in response to chromosome monoorientation is mediated by an inhibitory signal produced by unattached kinetochores. J. Cell Biol. *130*, 941–948.

Rowinsky, E.K., Eisenhauer, E.A., Chaudhry, V., Arbuck, S.G., and Donehower, R.C. (1993). Clinical toxicities encountered with paclitaxel (Taxol). Semin. Oncol. *20*, 1–15.

Sherwood, S.W., Sheridan, J.P., and Schimke, R.T. (1994). Induction of apoptosis by the anti-tubulin drug colcemid: relationship of mitotic checkpoint control to the induction of apoptosis in HeLa S3 cells. Exp. Cell Res. *215*, 373–379.

Shi, J., Orth, J.D., and Mitchison, T. (2008). Cell type variation in responses to antimitotic drugs that target microtubules and kinesin-5. Cancer Res. *68*, 3269–3276.

Shin, H.J., Baek, K.H., Jeon, A.H., Park, M.T., Lee, S.J., Kang, C.M., Lee, H.S., Yoo, S.H., Chung, D.H., Sung, Y.C., et al. (2003). Dual roles of human BubR1, a mitotic checkpoint kinase, in the monitoring of chromosomal instability. Cancer Cell *4*, 483–497.

Steen, J.A., Steen, H., Georgi, A., Parker, K., Springer, M., Kirchner, M., Hamprecht, F., and Kirschner, M.W. (2008). Different phosphorylation states of the anaphase promoting complex in response to antimitotic drugs: a quantitative proteomic analysis. Proc. Natl. Acad. Sci. USA *105*, 6069–6074.

Strebhardt, K., and Ullrich, A. (2006). Targeting polo-like kinase 1 for cancer therapy. Nat. Rev. Cancer *6*, 321–330.

Sudo, T., Nitta, M., Saya, H., and Ueno, N.T. (2004). Dependence of paclitaxel sensitivity on a functional spindle assembly checkpoint. Cancer Res. *64*, 2502–2508.

Tang, P.A., Siu, L.L., Chen, E.X., Hotte, S.J., Chia, S., Schwarz, J.K., Pond, G.R., Johnson, C., Colevas, A.D., Synold, T.W., et al. (2008). Phase II study of ispinesib in recurrent or metastatic squamous cell carcinoma of the head and neck. Invest. New Drugs *26*, 257–264.

Tao, W., South, V.J., Zhang, Y., Davide, J.P., Farrell, L., Kohl, N.E., Sepp-Lorenzino, L., and Lobell, R.B. (2005). Induction of apoptosis by an inhibitor of the mitotic kinesin KSP requires both activation of the spindle assembly checkpoint and mitotic slippage. Cancer Cell *8*, 49–59.

Tao, W., South, V.J., Diehl, R.E., Davide, J.P., Sepp-Lorenzino, L., Fraley, M.E., Arrington, K.L., and Lobell, R.B. (2007). An inhibitor of the kinesin spindle protein activates the intrinsic apoptotic pathway independently of p53 and de novo protein synthesis. Mol. Cell. Biol. *27*, 689–698.

Taylor, S.S., and McKeon, F. (1997). Kinetochore localization of murine Bub1 is required for normal mitotic timing and checkpoint response to spindle damage. Cell *89*, 727–735.

Thompson, S.L., and Compton, D.A. (2008). Examining the link between chromosomal instability and aneuploidy in human cells. J. Cell Biol. *180*, 665–672.

Tighe, A., Johnson, V.L., Albertella, M., and Taylor, S.S. (2001). Aneuploid colon cancer cells have a robust spindle checkpoint. EMBO Rep. *2*, 609–614.

Tighe, A., Johnson, V.L., and Taylor, S.S. (2004). Truncating APC mutations have dominant effects on proliferation, spindle checkpoint control, survival and chromosome stability. J. Cell Sci. *117*, 6339–6353.

Tighe, A., Ray-Sinha, A., Staples, O.D., and Taylor, S.S. (2007). GSK-3 inhibitors induce chromosome instability. BMC Cell Biol. *8*, 34.

Uetake, Y., and Sluder, G. (2004). Cell cycle progression after cleavage failure: mammalian somatic cells do not possess a "tetraploidy checkpoint". J. Cell Biol. *165*, 609–615.

Vogel, C., Kienitz, A., Hofmann, I., Muller, R., and Bastians, H. (2004). Crosstalk of the mitotic spindle assembly checkpoint with p53 to prevent polyploidy. Oncogene *23*, 6845–6853.

Wang, X., Jin, D.Y., Wong, H.L., Feng, H., Wong, Y.C., and Tsao, S.W. (2003). MAD2-induced sensitization to vincristine is associated with mitotic arrest and Raf/Bcl-2 phosphorylation in nasopharyngeal carcinoma cells. Oncogene *22*, 109–116.

Weaver, B.A., and Cleveland, D.W. (2005). Decoding the links between mitosis, cancer, and chemotherapy: The mitotic checkpoint, adaptation, and cell death. Cancer Cell *8*, 7–12.

Woods, C.M., Zhu, J., McQueney, P.A., Bollag, D., and Lazarides, E. (1995). Taxol-induced mitotic block triggers rapid onset of a p53-independent apoptotic pathway. Mol. Med. *1*, 506–526.